Geochemical Perspectives Letters

Dating recent aqueous activity on Mars

M.M. Tremblay[1*], D.F. Mark[2,3], D.N. Barfod[2], B.E. Cohen[2,4], R.B. Ickert[1], M.R. Lee[4], T. Tomkinson[5], C.L. Smith[4,6]

https://doi.org/10.7185/geochemlet.2443

Abstract

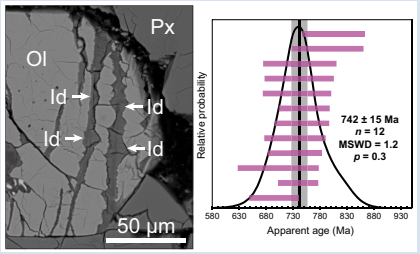

Amazonian-age Martian meteorites contain products of indigenous aqueous alteration; yet, establishing when this alteration occurred, and therefore when liquid water was available in the planet's crust, has proven challenging. New $^{40}Ar/^{39}Ar$ dates for iddingsite within the Martian meteorite Lafayette show these minerals precipitated from liquid water at 742 ± 15 Ma (2σ). This age is the most precise constraint to date on water–rock interaction on Mars, and postdates formation of the host igneous rock by ~580 Myr. We infer that magmatic activity most likely induced melting of local permafrost and led to alteration of the nakhlites, suggesting that activation of localised hydrological cycles on Amazonian Mars by magmatism was infrequent and transient, but not unusual.

Received 10 August 2024 | Accepted 15 October 2024 | Published 6 November 2024

Introduction

A key objective of ongoing and future missions to Mars is determining when the planet's hydrological cycle was active in the geologic past. For much of the Amazonian period (2.9 Ga to present), Mars's surface was cold and arid with a thin atmosphere, making liquid water unstable at the surface (*e.g.*, Carr and Head, 2010). However, minerals that formed by aqueous alteration of Amazonian-aged rocks, which have travelled to Earth as meteorites, show that liquid water was available at some points during this time period (Gooding *et al.*, 1991; Treiman *et al.*, 1993).

The nakhlite meteorites are a group of igneous rocks that crystallised between 1416 ± 4 and 1322 ± 5 Ma, and were subsequently ejected by an impact event at 10.7 ± 0.4 Ma (Cohen *et al.*, 2017). Several nakhlites contain aqueous alteration products (*e.g.*, Treiman, 2005) that (1) are crosscut by fusion crusts that formed upon atmospheric entry to Earth (*e.g.*, Gooding *et al.*, 1991; Treiman *et al.*, 1993) and (2) have D/H ratios indicative of fluid equilibration with the Martian atmosphere (Leshin *et al.*, 1996), requiring that these secondary phases formed *via* interaction of the igneous rocks with liquid water on Mars (*e.g.*, Leshin *et al.*, 1996).

Lafayette is one such member of the nakhlites. It is a 0.8 kg olivine-rich pyroxenite find with negligible evidence for terrestrial weathering (Graham *et al.*, 1985; Treiman *et al.*, 1993; Lee *et al.*, 2015). Olivine grains and the mesostasis of Lafayette host aqueous alteration products that include K-bearing hydrous silicates (*e.g.*, Piercy *et al.*, 2022, and references therein; see Supplementary Information). We refer to this alteration mineral assemblage as "iddingsite". The focus of the present study is to determine the age of iddingsite in the olivine-hosted veins (Fig. 1), which comprise 2.3–2.7 volume percent of Lafayette (Lee *et al.*, 2015).

The question of when Lafayette and the other nakhlites were exposed to liquid water on Mars remains unresolved. The most widely cited constraint derives from the Rb-Sr systematics of acid-leachates from the meteorites Lafayette and Yamato (Y) 000593 (Shih *et al.*, 1998; Misawa *et al.*, 2005). These experiments were designed to measure the isotopic systematics of the primary igneous minerals. The acid leach component was meant to remove the iddingsite and any terrestrial weathering products, but was not designed to extract chronological information. Nonetheless, these measurements have also been used to extract apparent, two-point isochron ages of 674 ± 68 Ma and 653 ± 80 Ma (2σ, recalculated; see Supplementary Information for Rb-Sr systematics and $^{40}Ar/^{39}Ar$ methods) for Lafayette (Shih *et al.*, 1998) and Y000593 (Misawa *et al.*, 2005), respectively. With an isochron defined by two points, there is no way to test for contamination or isotopic disturbance, the latter being particularly important as the leaching procedure may produce Rb/Sr fractionation (Clauer *et al.*, 1993). And while these two datasets have been aggregated to estimate a single 'date' for nakhlite alteration (Borg and Drake, 2005), they are not consistent with a single isochron (see Supplementary Information), which raises questions about the overall chronological significance of these data.

1. Department of Earth, Atmospheric, and Planetary Sciences, Purdue University, West Lafayette, IN, 47907, USA
2. Scottish Universities Environmental Research Centre (SUERC), East Kilbride, G75 0QF, UK
3. Department of Earth & Environmental Science, University of St Andrews, St Andrews, KY16 9AJ, UK
4. School of Geographical and Earth Sciences, University of Glasgow, Glasgow, G12 8QQ, UK
5. School of Earth Sciences, University of Bristol, Bristol, BS8 1RJ, UK
6. Science Group, The Natural History Museum, London, SW7 5BD, UK
* Corresponding author (email: tremblam@purdue.edu)

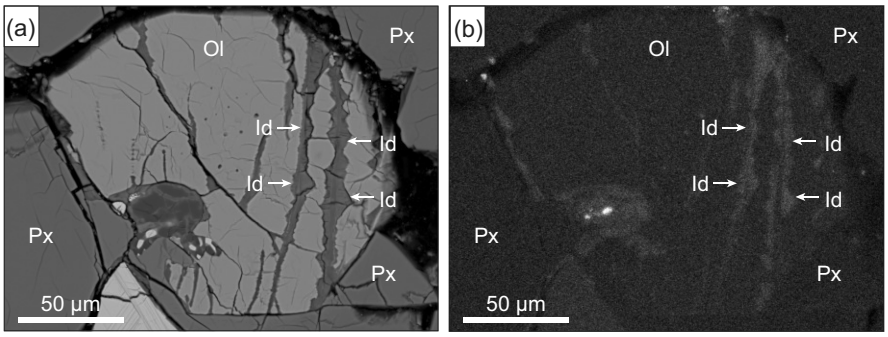

Figure 1 Petrographic context of Lafayette iddingsite. **(a)** Backscattered electron image showing an olivine grain (Ol) surrounded by augite crystals (Px) and cut by iddingsite-filled veins (Id). **(b)** Energy Dispersive Spectroscopy (EDS) X-ray map showing potassium enrichment (brighter grey) in iddingsite. Data were collected using a Carl Zeiss Sigma scanning electron microscope (SEM) at the University of Glasgow, operated in high-vacuum mode at 20 kV and ~2 nA.

Previous work applying the ^{40}K-^{40}Ar chronometer to Lafayette is also ambiguous, suggesting that the nakhlites interacted with aqueous fluids sometime between 670 and 0 Ma (Swindle *et al.*, 2000). These dates were likely impacted by inhomogeneous K distribution between the distinct aliquots of material measured for their ^{40}K and ^{40}Ar content.

Methods

We revisited the age of iddingsite in Lafayette using the ^{40}Ar/^{39}Ar technique, a variant of the ^{40}K-^{40}Ar dating method used by Swindle *et al.* (2000). We obtained 0.216 g of Lafayette from the Smithsonian Institution, sourced from an interior core >20 cm from the fusion crust. Iddingsite was physically separated from the host olivine (see Supplementary Information). During the neutron irradiation required for ^{40}Ar/^{39}Ar dating, the ^{39}Ar atoms produced recoil with an average distance of 0.08 µm in silicate minerals (Turner and Cadogan, 1974). Thus, fine-grained materials with high surface area-to-volume ratios, like the iddingsite studied here, may lose ^{39}Ar during the irradiation process, resulting in spuriously old ages (Onstott *et al.*, 1995). The dating of fine-grained materials using the ^{40}Ar/^{39}Ar technique thus requires a non-conventional approach, which consists of micro-encapsulation to prevent loss of recoiled isotopes (Dong *et al.*, 1997). To achieve this, we encapsulated twelve ~1 µg aliquots of the hand-picked iddingsite in evacuated, flame-sealed quartz glass capsules prior to neutron irradiation. Following irradiation, we measured the Ar isotopic composition of the iddingsite in two stages. First, the glass capsule was cracked under vacuum to measure any recoiled ^{37}Ar and ^{39}Ar. Second, the samples recovered from the cracked glass tubes were then fused with a diode laser. The ^{37}Ar and ^{39}Ar measurements from the cracked tubes were added to the total fusion isotope measurements (^{36}Ar, ^{37}Ar, ^{38}Ar, ^{39}Ar, and ^{40}Ar). Data were corrected for backgrounds, mass discrimination, radioactive decay since irradiation, cosmogenic Ar, and trapped Martian atmospheric Ar. Full analytical procedure details are provided in the Supplementary Information.

Results

Upon cracking the quartz capsules, we observed that significant ^{39}Ar and ^{37}Ar recoil occurred during neutron irradiation into the quartz capsule of 16 ± 2 % and 13 ± 2 %, respectively. When the Ar isotopic data from the two-stage analytical procedure are combined, the data define a normal age distribution with a mean ^{40}Ar/^{39}Ar age of 741.8 ± 15.0/15.2 Ma (analytical precision/full external precision at 2σ). There is no statistically significant difference between the individual aliquot ages, defining a mean square weighted deviation (MSWD) of 1.2 and a *p*-value of 0.3 (Fig. 2). This age for the iddingsite in Lafayette agrees within uncertainty with the previously estimated age from Rb-Sr acid-leachates (Shih *et al.*, 1998) but is significantly more precise. It is slightly older than the wide age range previously estimated from K-Ar measurements (Swindle *et al.*, 2000).

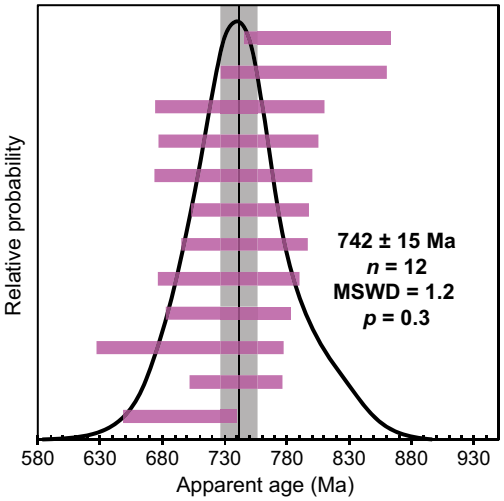

Figure 2 Rank age (purple bars, 2σ) and relative probability (black curve) of ^{40}Ar/^{39}Ar dates for 12 aliquots of Lafayette iddingsite. The data define a Gaussian distribution and indicate no scatter beyond what is expected from measurement precision.

Discussion

Potential for diffusive loss of Ar. Because we conducted total fusion ^{40}Ar/^{39}Ar measurements on the iddingsite aliquots, we did not recover information about the spatial distribution of radiogenic ^{40}Ar in the constituent phases. Therefore, we must evaluate the possibility that the aqueous alteration in Lafayette occurred earlier than 742 Ma, and that heating events at 742 Ma, or later, caused partial loss of radiogenic ^{40}Ar. The maximum possible ^{40}Ar loss is 44 %, based on the difference between the measured iddingsite age and Lafayette's igneous crystallisation age (~1322 Ma; Cohen *et al.*, 2017).

The bulk ^{40}Ar/^{39}Ar systematics of the nakhlites reported by Cohen *et al.* (2017) preclude protracted heating of Lafayette

during its residence in Mars's crust. Therefore, we consider three aspects of Lafayette's history that could have induced ^{40}Ar loss: (1) heating during an impact event, such as the impact that ejected Lafayette from Mars *ca*. 10.7 Ma; (2) heating during Lafayette's transit in space before falling to Earth; and (3) heating during entry into Earth's atmosphere. To assess the influence of heating during these events on the ^{40}Ar/^{39}Ar age, we modelled the diffusive loss of Ar from iddingsite. Following others who have applied ^{40}Ar/^{39}Ar dating to authigenic clays (*e.g.*, Clauer *et al.*, 2003), we assume the diffusion kinetics of Ar in muscovite are comparable to those in the K-bearing phases comprising iddingsite and use the kinetic parameters for Ar diffusion in muscovite reported by Harrison *et al.* (2009). The grain size of the iddingsite in Lafayette is not well constrained, but it cannot be greater than 10–20 μm based on the width of the olivine-hosted veins. We therefore explored models with diffusion radii between 0.01 and 10 μm, assuming the grain size defines the diffusion length scale.

In the case of the 10.7 Ma impact event and/or atmospheric entry, we use approximations for fractional loss during a square pulse heating event (Fig. 3a; see Supplementary Information). The duration of heating for both events is geologically brief: up to several hours after ejection (*e.g.*, Fritz *et al.*, 2005) or hundreds of seconds during atmospheric entry (*e.g.*, Parnell *et al.*, 2008). For these scenarios, we therefore assume radiogenic ^{40}Ar production during heating is negligible. However, in the case of Lafayette's 10.7 Myr transit in space, the production of radiogenic ^{40}Ar is nontrivial. We therefore use a solution for radiogenic ^{40}Ar production and diffusive loss during an isothermal heating event, which incorporates the initial age prior to heating. Although Lafayette's temperature would have varied as it transited the inner Solar System, we use the isothermal heating solution as an end member to estimate the minimum temperatures that would yield diffusive loss (Fig. 3b; see Supplementary Information).

For an impact and atmospheric entry, temperatures >~250 °C would need to be sustained for several days, or longer, for Ar loss to exceed 1 % (Fig. 3a). Lower temperatures are required for Ar loss during space transit due to its longer duration (Fig. 3b). For example, for a grain radius of 0.01 μm, temperatures would need to exceed ~160 °C for >1 % diffusive loss of Ar to take place. Higher temperatures during space transit are permitted without diffusive loss over durations <10.7 Myr.

When paired with other observations, these first-order thermal constraints suggest that an age for the Lafayette iddingsite significantly older than 742 Ma age is highly unlikely. For heating during impact ejection, independent estimates based on the shock petrography of Lafayette indicate that shock and post-shock temperatures were at most several tens of degrees Celsius above ambient Martian surface temperatures (*e.g.*, Fritz *et al.*, 2005; Daly *et al.*, 2019). Following ejection, the maximum temperatures that Lafayette could have experienced during space transit are 200–250 °C, which would occur if its orbit approached Mercury (Butler, 1966). However, orbital dynamics calculations demonstrate that a prolonged duration near Mercury is extremely unlikely for a Martian meteorite that falls to Earth (*e.g.*, Gladman, 1997). Therefore, Lafayette likely spent most, or all, of its 10.7 Myr space transit at temperatures well below those required to cause Ar loss (150–200 °C; Fig. 3b). Finally, we expect heating during atmospheric entry to be insignificant, considering that our samples were sourced ~20 cm from Lafayette's fusion crust. The Stone 5 experiments, which placed rocks on the nose of a spacecraft to simulate atmospheric entry, only documented re-entry heating >100 °C at <2 cm depth below the rocks' fusion crust (Parnell *et al.*, 2008). Collectively, these observations and our calculations indicate that while partial Ar loss from Lafayette iddingsite is possible under certain conditions, it is very unlikely given other constraints about Lafayette's history.

Significance of the ^{40}Ar/^{39}Ar age. Given that (1) the ^{40}Ar/^{39}Ar data show no significant scatter beyond what is expected from the measurement precision, (2) radiogenic ^{40}Ar loss from the Lafayette iddingsite is highly unlikely, and (3) the new ^{40}Ar/^{39}Ar date is broadly consistent with previous but significantly less precise age estimates, we interpret the ^{40}Ar/^{39}Ar age of 742 ± 15 Ma as recording the time when the iddingsite in Lafayette formed as a result of water–rock interaction close to the surface of Mars.

Our data show that the impact event recorded by Nakhla at ~913 Ma (Cassata *et al.*, 2010) was not coeval with the aqueous activity that led to iddingsite formation in Lafayette. The impact

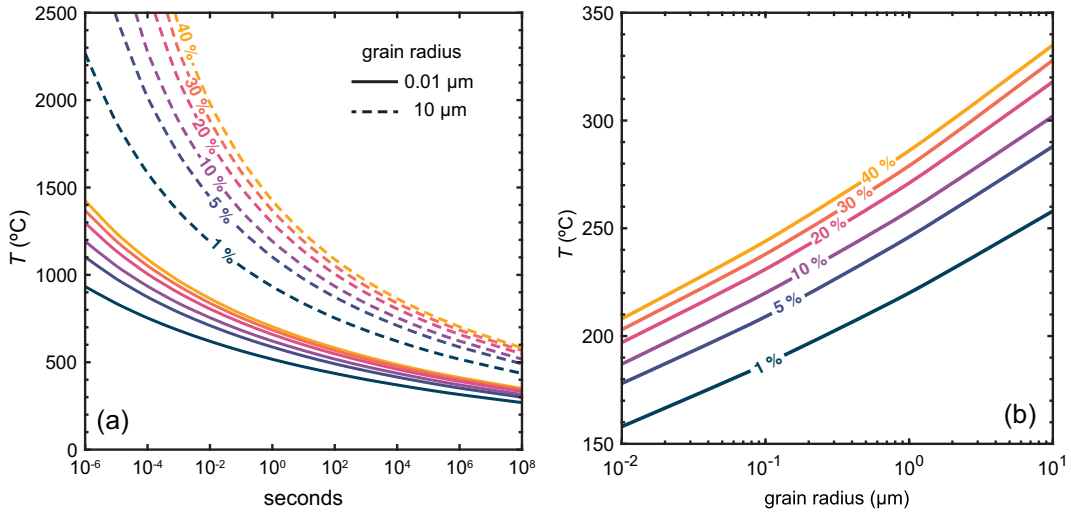

Figure 3 Thermal limits on Ar diffusive loss from Lafayette iddingsite. **(a)** Argon fractional loss (0–40 %) as a function of duration and temperature of a square pulse heating event, such as during an impact or atmospheric entry, for two different end member iddingsite grain sizes. **(b)** Argon fractional loss as a function of grain size and temperature for an isothermal heating event lasting 10.7 Myr, the duration of Lafayette's transit in space (Cohen *et al.*, 2017).

event at 913 Ma is the only evidence that the nakhlites have experienced impact-induced shock following cooling of the parent lavas and prior to their ejection at 10.7 Ma. The impact event at 913 Ma was likely responsible for producing the shock features in Lafayette documented by Daly *et al.* (2019), and for increasing the porosity and permeability for later aqueous solutions to infiltrate grain interiors within Lafayette at 742 Ma (Lee *et al.*, 2015), but did not induce the aqueous alteration of Lafayette or the nakhlites directly. The data do not preclude the occurrence of a third impact event at 742 Ma. However, such an event would have to be low enough energy to not disturb the Ar isotope systematics of primary phases in the nakhlites, but high enough energy to induce subsurface melting of localised permafrost, providing the heat source for water–rock interaction that led to alteration of the nakhlites (*e.g.*, Changela and Bridges, 2010). Moreover, it is unlikely that three large impact events occurred at the same place on the Martian surface during the last 1 Ga (*ca*. 913 Ma, 742 Ma, 10.7 Ma).

An alternate and simpler explanation is that magmatism acted as a localised heat source for melting of subsurface ice and water–rock interaction during the Amazonian on Mars. On Earth, iddingsite is commonly observed in olivine grains of igneous rocks that experience post-emplacement hydrothermal activity not linked to impact cratering (*e.g.*, Carlson and Rodgers, 1975), so it is reasonable to infer a similar process happening on Mars. The spatial variability of alteration within the nakhlites (Lee *et al.*, 2015) is consistent with a model of heat from magmatic eruptions or intrusions at ~742 Ma, inducing localised, short-lived melting of permafrost. Such spatial variability is diagnostic of a small-scale hydrologic system, whereas higher water to rock ratios, and more pervasive alteration, are more commonly associated with an allochemical, impact-driven hydrothermal cell (Bridges and Schwenzer, 2012). A model for a short-lived heat source of magmatic origin is thus congruent with the low temperature models for nakhlite alteration proposed previously (*e.g.*, Treiman *et al.*, 1993). Fluid–rock interaction at ~742 Ma selectively widened and extended the fractures within olivine through carbonation (*e.g.*, Tomkinson *et al.*, 2013). The dissolution of the host olivine provides many of the cations required to precipitate the secondary minerals observed in the nakhlites (Lee *et al.*, 2015)—another key requirement of a highly localised, isochemical system. Similarly, the potassium found within the iddingsite (Fig. 1) was likely sourced locally from dissolution of feldspar and glass in the mesostasis (Bridges and Schwenzer, 2012).

The timing of iddingsite formation in Lafayette coincides with a volcanically active period of Mars's history, albeit eruption frequency was decreasing. Amazonian-age volcanism is restricted to the Tharsis and Elysium regions of Mars and their peripheries (Carr and Head, 2010); the nakhlites are most likely sourced from these regions (Herd *et al.*, 2024). Crater ages of tens of millions of years for volcanic surfaces in Tharsis and Elysium, including the crater that formed when the nakhlites were ejected, suggest that Mars is still episodically volcanically active.

Conclusions

The new $^{40}Ar/^{39}Ar$ geochronology presented here demonstrates that the timing for aqueous alteration of Martian volcanic rocks by water was unrelated to their emplacement or an impact event, but most likely related to ongoing magmatic activity on Mars *ca*. 742 Ma. Our proposed model is consistent with previous models for the alteration environment of the nakhlites. Considering the low eruption rate for Amazonian volcanoes and the prevalence of permafrost across Mars, our data support interpretations that activation of localised hydrological cycles on Amazonian Mars by magmatic activity was infrequent but not unusual.

Acknowledgements

Funding from UK Science and Technology Facilities Council (ST/H002472/1 and ST/H002960/1) is gratefully acknowledged. The sample we obtained from the Smithsonian was Lafayette USNM 1505. We thank R. Dymock and J. Imlach for assistance with micro-encapsulation $^{40}Ar/^{39}Ar$ dating, P. Chung for support with SEM observations, A. Fallick for advice on experiment design, J. Bridges and S. Schwenzer for fruitful discussion on nakhlite alteration, and D. Minton for discussion on meteorite orbits. Finally, we thank M. Martínez, A. Treiman, and two anonymous reviewers for their helpful feedback, as well as F. McCubbin for editorial handling.

Editor: Francis McCubbin

Additional Information

Supplementary Information accompanies this letter at https://www.geochemicalperspectivesletters.org/article2443.

Cite this letter as: Tremblay, M.M., Mark, D.F., Barfod, D.N., Cohen, B.E., Ickert, R.B., Lee, M.R., Tomkinson, T., Smith, C.L. (2024) Dating recent aqueous activity on Mars. *Geochem. Persp. Let.* 32, 58–62. https://doi.org/10.7185/geochemlet.2443

References

Borg, L., Drake, M.J. (2005) A review of meteorite evidence for the timing of magmatism and of surface or near-surface liquid water on Mars. *Journal of Geophysical Research: Planets* 110, E12S03. https://doi.org/10.1029/2005JE002402

Bridges, J.C., Schwenzer, S.P. (2012) The nakhlite hydrothermal brine on Mars. *Earth and Planetary Science Letters* 359–360, 117–123. https://doi.org/10.1016/j.epsl.2012.09.044

Butler, C.P. (1966) Temperatures of Meteoroids in Space. *Meteoritics* 3, 59–70. https://doi.org/10.1111/j.1945-5100.1966.tb00355.x

Carlson, J.R., Rodgers, K.A. (1975) The petrology and alteration of tertiary basalts of the coalgate area, Northwest Canterbury. *Journal of the Royal Society of New Zealand* 5, 195–205. https://doi.org/10.1080/03036758.1975.10419372

Carr, M.H., Head III, J.W. (2010) Geologic history of Mars. *Earth and Planetary Science Letters* 294, 185–203. https://doi.org/10.1016/j.epsl.2009.06.042

Cassata, W.S., Shuster, D.L., Renne, P.R., Weiss, B.P. (2010) Evidence for shock heating and constraints on Martian surface temperatures revealed by $^{40}Ar/^{39}Ar$ thermochronometry of Martian meteorites. *Geochimica et Cosmochimica Acta* 74, 6900–6920. https://doi.org/10.1016/j.gca.2010.08.027

Changela, H.G., Bridges, J.C. (2010) Alteration assemblages in the nakhlites: Variation with depth on Mars. *Meteoritics & Planetary Science* 45, 1847–1867. https://doi.org/10.1111/j.1945-5100.2010.01123.x

Clauer, N., Chaudhuri, S., Kralik, M., Bonnot-Courtois, C. (1993) Effects of experimental leaching on Rb-Sr and K-Ar isotopic systems and REE contents of diagenetic illite. *Chemical Geology* 103, 1–16. https://doi.org/10.1016/0009-2541(93)90287-S

Clauer, N., Zwingmann, H., Gorokhov, I.M. (2003) Postdepositional Evolution of Platform Claystones Based on a Simulation of Thermally Induced Diffusion of Radiogenic ^{40}Ar from Diagenetic Illite. *Journal of Sedimentary Research* 73, 58–63. https://doi.org/10.1306/061002730058

Cohen, B.E., Mark, D.F., Cassata, W.S., Lee, M.R., Tomkinson, T., Smith, C.L. (2017) Taking the pulse of Mars via dating of a plume-fed volcano. *Nature Communications* 8, 640. https://doi.org/10.1038/s41467-017-00513-8

Daly, L., Lee, M.R., Piazolo, S., Griffin, S., Bazargan, M., Campanale, F., Chung, P., Cohen, B.E., Pickersgill, A.E., Hallis, L.J., Trimby, P.W., Baumgartner, R., Forman, L.V., Bendix, G.K. (2019) Boom boom pow: Shock-facilitated aqueous alteration and evidence for two shock events in the Martian nakhlite meteorites. *Science Advances* 5, eaaw5549. https://doi.org/10.1126/sciadv.aaw5549

Dong, H., Hall, C.M., Halliday, A.N., Peacor, D.R., Merriman, R.J., Roberts, B. (1997) ^{40}Ar/^{39}Ar illite dating of Late Caledonian (Acadian) metamorphism and cooling of K-bentonites and slates from the Welsh Basin, U.K. *Earth and Planetary Science Letters* 150, 337–351. https://doi.org/10.1016/S0012-821X(97)00100-3

Fritz, J., Artemieva, N., Greshake, A. (2005) Ejection of Martian meteorites. *Meteoritics & Planetary Science* 40, 1393–1411. https://doi.org/10.1111/j.1945-5100.2005.tb00409.x

Gladman, B. (1997) Destination: Earth. Martian Meteorite Delivery. *Icarus* 130, 228–246. https://doi.org/10.1006/icar.1997.5828

Gooding, J.L., Wentworth, S.J., Zolensky, M.E. (1991) Aqueous alteration of the Nakhla meteorite. *Meteoritics* 26, 135–143. https://doi.org/10.1111/j.1945-5100.1991.tb01029.x

Graham, A.L., Hutchison, R., Bevan, A.W.R. (1985) *Catalogue of meteorites*. Fourth Edition, University of Arizona Press, Tucson.

Harrison, T.M., Célérier, J., Aikman, A.B., Hermann, J., Heizler, M.T. (2009) Diffusion of ^{40}Ar in muscovite. *Geochimica et Cosmochimica Acta* 73, 1039–1051. https://doi.org/10.1016/j.gca.2008.09.038

Herd, C.D.K., Hamilton, J.S., Walton, E.L., Tornabene, L.L., Lagain, A., Benedix, G.K., Sheen, A.I., Melosh, H.J., Johnson, B.C., Wiggins, S.E., Sharp, T.G., Darling, J.R. (2024) The source craters of the martian meteorites: Implications for the igneous evolution of Mars. *Science Advances* 10, eadn2378. https://doi.org/10.1126/sciadv.adn2378

Lee, M.R., Tomkinson, T., Hallis, L.J., Mark, D.F. (2015) Formation of iddingsite veins in the martian crust by centripetal replacement of olivine: Evidence from the nakhlite meteorite Lafayette. *Geochimica et Cosmochimica Acta* 154, 49–65. https://doi.org/10.1016/j.gca.2015.01.022

Leshin, L.A., Epstein, S., Stolper, E.M. (1996) Hydrogen isotope geochemistry of SNC meteorites. *Geochimica et Cosmochimica Acta* 60, 2635–2650. https://doi.org/10.1016/0016-7037(96)00122-6

Misawa, K., Shih, C.-Y., Wiesmann, H., Garrison, D.H., Nyquist, L.E., Bogard, D.D. (2005) Rb-Sr, Sm-Nd and Ar-Ar isotopic systematics of Antarctic nakhlite Yamato 000593. *Antarctic Meteorite Research* 18, 133–151.

Onstott, T.C., Miller, M.L., Ewing, R.C., Arnold, G.W., Walsh, D.S. (1995) Recoil refinements: Implications for the ^{40}Ar/^{39}Ar dating technique. *Geochimica et Cosmochimica Acta* 59, 1821–1834. https://doi.org/10.1016/0016-7037(95)00085-E

Parnell, J., Mark, D., Brandstätter, F. (2008) Response of sandstone to atmospheric heating during the STONE 5 experiment: Implications for the palaeofluid record in meteorites. *Icarus* 197, 282–290. https://doi.org/10.1016/j.icarus.2008.04.014

Piercy, J.D., Bridges, J.C., Hicks, L.J. (2022) Carbonate dissolution and replacement by odinite and saponite in the Lafayette nakhlite: Part of the CO_2-CH_4 cycle on Mars? *Geochimica et Cosmochimica Acta* 326, 97–118. https://doi.org/10.1016/j.gca.2022.02.003

Shih, C.-Y., Nyquist, L.E., Reese, Y., Wiesmann, H. (1998) The Chronology of the Nakhlite, Lafayette: Rb-Sr and Sm-Nd Isotopic Ages. *Lunar and Planetary Science Conference XXIX*, abstract 1145.

Swindle, T.D., Treiman, A.H., Lindstrom, D.J., Burkland, M.K., Cohen, B.A., Grier, J.A., Li, B., Olson, E.K. (2000) Noble gases in iddingsite from the Lafayette meteorite: Evidence for liquid water on Mars in the last few hundred million years. *Meteoritics & Planetary Science* 35, 107–115. https://doi.org/10.1111/j.1945-5100.2000.tb01978.x

Tomkinson, T., Lee, M.R., Mark, D.F., Smith, C.L. (2013) Sequestration of Martian CO_2 by mineral carbonation. *Nature Communications* 4, 2662. https://doi.org/10.1038/ncomms3662

Treiman, A.H. (2005) The nakhlite meteorites: Augite-rich igneous rocks from Mars. *Geochemistry* 65, 203–270. https://doi.org/10.1016/j.chemer.2005.01.004

Treiman, A.H., Barrett, R.A., Gooding, J.L. (1993) Preterrestrial aqueous alteration of the Lafayette (SNC) meteorite. *Meteoritics* 28, 86–97. https://doi.org/10.1111/j.1945-5100.1993.tb00251.x

Turner, G., Cadogan, P.H. (1974) Possible effects of ^{39}Ar recoil in ^{40}Ar-^{39}Ar dating. *Proceedings of the Fifth Lunar Conference* 2, 1601–1615.

Geochemical Perspectives Letters

Dating recent aqueous activity on Mars

M.M. Tremblay, D.F. Mark, D.N. Barfod, B.E. Cohen, R.B. Ickert, M.R. Lee, T. Tomkinson, and C.L. Smith

Supplementary Information

The Supplementary Information includes:

- Alteration Phases in Lafayette
- Recalculation and Reinterpretation of Rb-Sr Systematics in Martian Meteorites Lafayette and Yamato (Y) 000593
- Micro-encapsulation $^{40}Ar/^{39}Ar$ Methods
- Argon Diffusion Calculations
- Figures S-1 to S-3
- Tables S-1 to S-3
- Supplementary Information References

Alteration Phases in Lafayette

The alteration phases present in Lafayette, which we collectively refer to as "iddingsite," and in the nakhlite meteorites more generally, have been extensively studied and described (*e.g.*, Bridges and Grady, 2000; Bridges *et al.*, 2019; Changela and Bridges, 2010; Gyollai *et al.*, 2023; Hicks *et al.*, 2014; Krämer Ruggiu *et al.*, 2020; Lee *et al.*, 2013, 2015, 2018; Martínez *et al.*, 2023; McCubbin *et al.*, 2009; Piercy *et al.*, 2022; Tomkinson *et al.*, 2013; Treiman, 2005; Treiman *et al.*, 1993). Here, we summarize some of the key mineralogical and textural observations that are of relevance for understanding our $^{40}Ar/^{39}Ar$ dates of the alteration phases in Lafayette.

The abundance, and to a lesser degree the mineralogy, of the alteration phases in Lafayette are documented to be variable across different samples or aliquots of the meteorite (*e.g.*, Piercy *et al.*, 2022). The aliquots of iddingsite that we separated for $^{40}Ar/^{39}Ar$ geochronology were taken from the same material that Tomkinson *et al.* (2013) and Lee *et al.* (2015) studied, so we focus on their characterization here. They documented that both narrow (1-2 μm) and wide (up to 40 μm) olivine-hosted veins contain finely crystallised Fe-Mg silicate identified as saponite (Tomkinson *et al.*, 2013). In the wider veins, the saponite is observed to be mantled by Fe-rich smectite phyllosilicates (*e.g.*, Treiman *et al.*, 1993) or intergrown smectite and serpentine (*e.g.*, Changela and Bridges, 2010), and in some of the widest veins siderite is also observed (*e.g.*, Tomkinson *et al.*, 2013; Lee *et al.*, 2015). Lee *et al.* (2015) interpreted the mineral assemblage in the olivine-hosted veins to reflect a multistage process, with the saponite crystallising and filling in fractures first, followed by the incongruent dissolution of the vein walls and replacement by siderite, which was finally replaced by the smectite or intergrown smectite and serpentine. While we were not able to differentiate between these major alteration phases when we physically separated the vein-filling alteration material from their olivine grain hosts, we anticipate based on mineralogy that the phyllosilicates will dominate the K budget responsible for production of radiogenic ^{40}Ar.

A multi-stage formation history of the iddingsite mineral assemblage in Lafayette (*e.g.*, Lee *et al.*, 2015) is consistent with detailed petrologic studies of the alteration assemblages in other nakhlites (*e.g.*, Changela and Bridges, 2010; Lee *et al.*, 2013; Gyollai *et al.*, 2023; Martínez *et al.*, 2023). Although we report the most precise date for these alteration phases in Lafayette to date, it is worth noting that the age we obtain of 742 Ma still has a nontrivial uncertainty of 15 Ma (2σ). Therefore, a multi-stage formation history of the alteration mineral assemblage is certainly permissible within the age window and could be significantly shorter (*e.g.*, Changela and Bridges, 2010), but this possibility is not currently resolvable *via* radiometric dating alone.

Recalculation and Reinterpretation of Rb-Sr Systematics in Martian Meteorites Lafayette and Yamato (Y) 000593

The most widely cited constraint on the timing of iddingsite formation in the nakhlites derives from the Rb-Sr systematics of acid-leachates from the meteorites Lafayette and Yamato (Y) 000593 (Shih *et al.*, 1998; Misawa *et al.*, 2005). The Rb-Sr data from Lafayette were only presented in a small figure in an abstract (Shih *et al.*, 1998). To reevaluate these data, we digitized the Rb-Sr data, as well as the Sm-Nd data, from the figures in Shih *et al.* (1998), including the uncertainties. Because the Rb-Sr data for Lafayette and Y000593 were combined by Borg and Drake (2005) to infer an age for iddingsite in the nakhlites, we also re-reduced the radioisotopic data (Rb-Sr and Sm-Nd) from both Lafayette (Shih *et al.*, 1998) and Y000593 (Misawa *et al.*, 2005) using a consistent calculation approach.

The radioisotopic data from Shih *et al.* (1998) were derived from a crushed, 0.5 g sample of Lafayette. We briefly summarize their methods here. Before separation, three whole rock aliquots (WR, WR1, WR2) were separated from the crushed sample. After WR separation, a pyroxene (Px) and an olivine (Ol) separate were picked by hand, as were two different "iddingsite" fragments (Id1 and Id2; described as a composite mixture of alteration materials, olivine and pyroxene). All aliquots except WR1 and WR2 were leached in 1 mol/L HCl. All leachates and residues, and the two unleached WR aliquots, were measured for their Rb, Sr, and Sr isotopic compositions. The methods used by Misawa *et al.* (2005) are very similar, with the exception that they used 2 mol/L HCl.

Digitization and new calculations of Rb-Sr and Sm-Nd systematics

There are line elements behind the data points in the vector figure of Shih *et al.* (1998) that we interpret as uncertainty bars. We interpret the uncertainties to be plotted at the 2σ level, because they are similar in magnitude to the reported 2σ uncertainties in Shih *et al.* (1999) on the nakhlite Governador Valadares, which were made using the same analytical methods in the same lab at around the same time. These values are reported in Table S-1. The original isochron-style regressions used what are now outdated implementations of line-fitting algorithms that are difficult or impossible to reproduce, and which may have been adjusted in ways that are not well documented (*cf.* discussion in Nyquist *et al.*, 1986). As a result, we have recalculated linear fits using a widely used and reproducible algorithm from York *et al.*, (2004). This algorithm underpins the default line-fitting method in Isoplot (Ludwig, 2008) and IsoplotR (Vermeesch, 2018). The uncertainties we report are based on propagating the *a priori* analytical uncertainties only, and no adjustment has been made to account for overdispersion. To compare our calculations to the originally reported values, we use the decay constants from the original publications ($\lambda_{87Rb} = 1.390 \cdot 10^{-11}$ a^{-1} for Shih *et al.* (1998) and $1.402 \cdot 10^{-11}$ a^{-1} for Misawa *et al.* (2005); and $\lambda_{147Sm} = 6.540 \cdot 10^{-12}$ a^{-1} for both). The difference between ages calculated with the two ^{87}Rb decay constants is ~11 Myr.

Using the digitized data for Lafayette and excluding the leachates from Id1 and Id2, as was done by Shih *et al.* (1998), the Rb-Sr data yield a line with a slope corresponding to a date of 1.281 ± 0.021 Ga and an intercept of 0.70259 ± 0.00004 (2σ; n = 10; MSWD = 23.4; Fig. S-1), compared to the published values of 1.26 ± 0.07 Ga and 0.70260 ± 0.00014 (no sigma level or MSWD were originally reported). To confirm the accuracy of our digitization, we also calculate an Sm-Nd age and intercept from the digitized data of 1.317 ± 0.033 Ga (2σ; n = 11; MSWD = 2.3) and initial

εNd of 16.3 ± 0.6, compared to the published values of 1.32 ± 0.05 Ga and initial εNd of 16.3 ± 0.4 (Shih *et al.*, 1998). These new values are summarized in Table S-1.

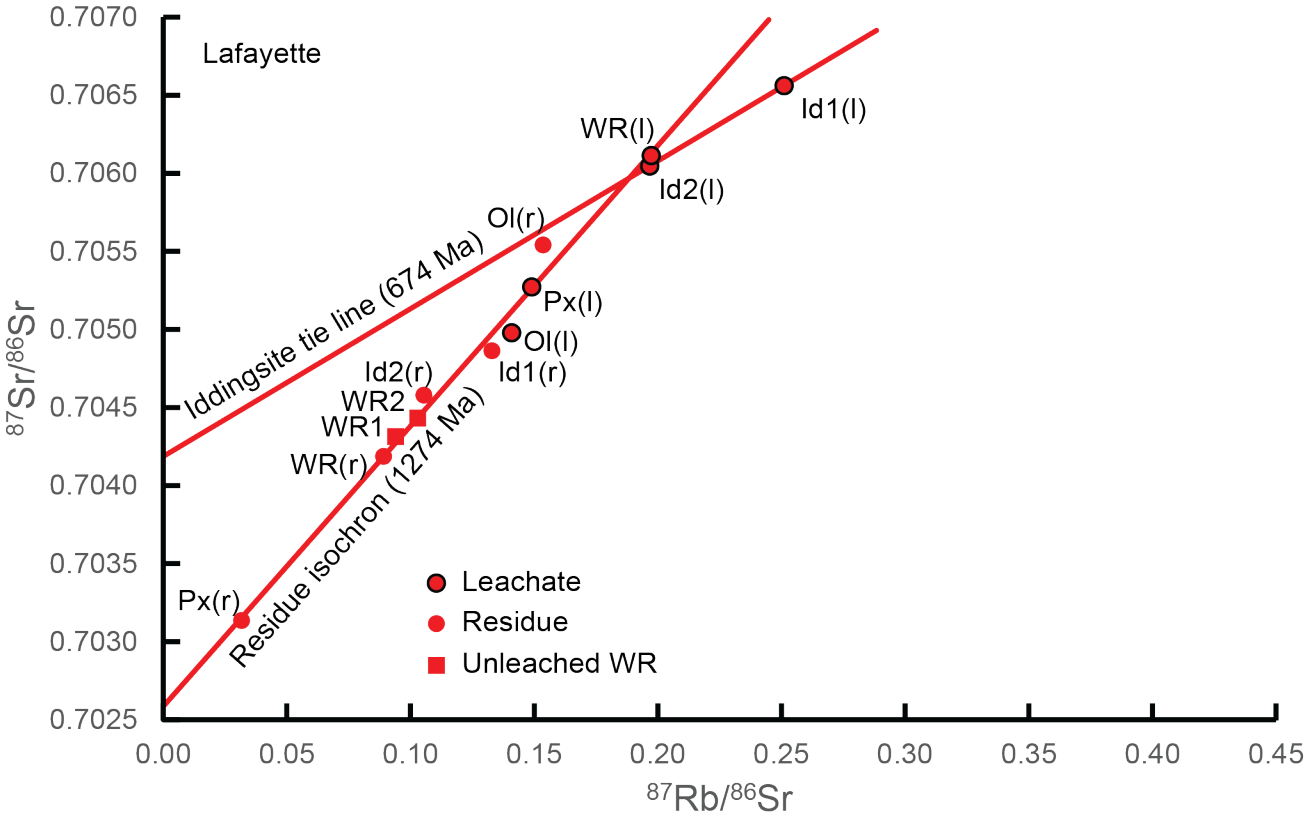

Figure S-1 Isochron style plot of Rb-Sr data from the meteorite Lafayette. Data has been digitized from the original figure of Shih *et al.* (1998). Uncertainties are smaller than the symbols plotted.

For consistency, we also re-reduced the data from Misawa *et al.* (2005) on Y000593. Using the same 5 aliquots for Rb-Sr as the authors (WR1, WR(r), Cpx(r), Cpx2(r), and NMag(r)), we calculate a line with a slope corresponding to a date of 1.302 ± 0.024 Ga and an intercept of 0.702524 ± 0.000027 (2σ; n = 5; MSWD = 3.1; Fig. S-1) compared with the published values of 1.30 ± 0.02 Ga and 0.702525 ± 0.000027 (no sigma level). For Sm-Nd, we use the same 6 samples as the authors (WR1, WR(r), WR(l), Cpx(r), Cpx(l), and Cpx2(r)) and recover a line with a slope corresponding to a date of 1.314 ± 0.018 Ga and initial εNd of 15.8 ± 0.4 (2σ; n = 6; MSWD = 4.8), compared to the published values of 13.1 ± 0.03 Ga and 16.0 ± 0.2 (no sigma level reported). These new values are summarized in Table S-1.

The results from the digitized data agree with the results presented by Shih *et al.* (1998) for Lafayette and for Y000593 presented by Misawa *et al.* (2005), which suggests that the digitization is broadly accurate. The larger uncertainties for some aliquots in the original publications appear to scale with the degree of overdispersion, and most likely are derived from an undescribed effort to account for non-analytical scatter (*cf.* Nyquist *et al.*, 1986). Calculating an MSWD makes clear that the Rb-Sr data of Lafayette are significantly overdispersed, implying a disturbance in the Rb-Sr systematics.

Reinterpretation of the Rb-Sr Systematics

The chronological information on timing of alteration of the nakhlites has previously been derived from four analyses, two each from Lafayette and Y000593 (Borg and Drake, 2005). From Lafayette, the two leachates were from separates

Id1 and Id2, the composite mixtures of primary igneous minerals and alteration material. From Y000593, the leachates are from two olivine separates, one from the 3.6-3.95 g/cm^3 fraction (Ol(l)), and one from the fraction denser than 3.95 g/cm^3, called ρ > 3.95. Each pair was regressed as a two-point model isochron. Recalculating a slope and intercept from each data pair yields apparent dates and initial Sr isotope compositions, at 2σ, of 677 ± 68 Ma and 0.7042 ± 0.0002 for Lafayette, and 650 ± 80 Ma and 0.7046 ± 0.0001 for Y000593. These recalculated values agree well with the original published values of 679 ± 66 Ma and 650 ± 80 Ma, respectively. Calculating the ages relative to a common decay constant (Rotenberg *et al.*, 2012) yields 674 ± 68 Ma for Lafayette and 653 ± 80 Ma for Y000593 (Figs. S-1 and S-2). Note that the Borg and Drake (2005) compilation also includes an additional date from Y000593 of 614 ± 29 Ma from the olivine residues based on a preliminary presentation of the data in an abstract (Shih *et al.*, 2002). However, the residual data later updated in Misawa *et al.* (2005) cannot be interpreted that way: the two olivine residue pairs have a negative slope on an isochron-style plot. Unfortunately, the uncorrected data from the residues reported originally (Shih *et al.*, 2002) were included as the most precise value in the weighted mean age for alteration in the nakhlites reported by Borg and Drake (2005), and therefore dominates their value.

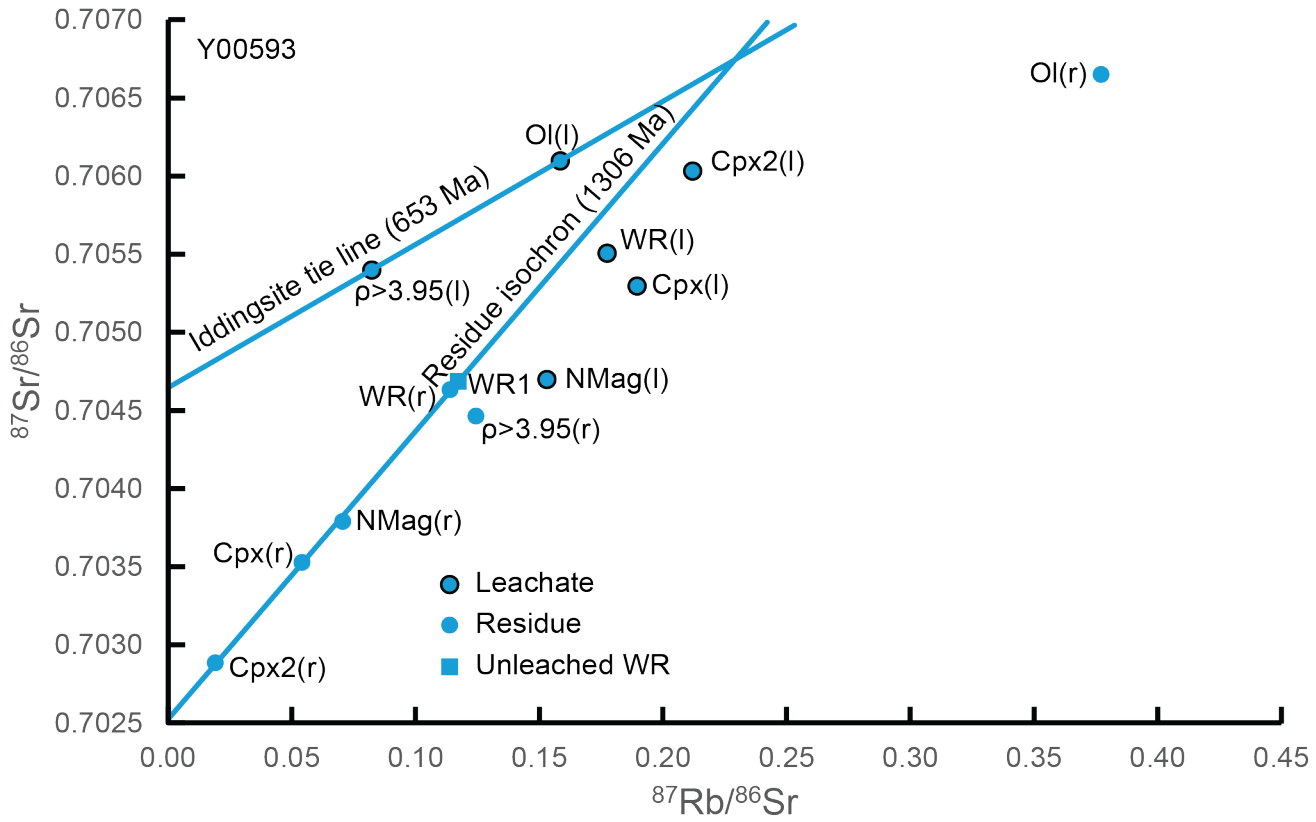

Figure S-2 Isochron style plot of Rb-Sr data from the meteorite Y000593. Data are from Misawa *et al.* (2005). Uncertainties are smaller than the symbols plotted.

There is no discussion of the chronological significance of the Lafayette two-point tie line apparent date in Shih *et al.* (1998). It is notable that the leached olivine separate from Lafayette, Ol(l), which presumably also contains iddingsite, does not plot near the slope of the Id1(l)-Id2(l) tie line (Fig. S-1). In Misawa *et al.* (2005), the discussion of Y000593 is framed speculatively, putting the word age, when associated with this two-point isochron, in quotation marks.

A two point model isochron provides no indication as to whether the Rb-Sr system has been disturbed. The only firm constraints provided by such a model are whether the data are non-physical, such if the linear fit had a negative

slope, or unlikely, such as if the linear fit had a slope in excess of 0.066, which would indicate a presolar date, or correspond to an impossible or unlikely intercept (*e.g.*, $^{87}Sr/^{86}Sr < 0.698$). Beyond these constraints, two-point linear fits allow for a wide range of possible Rb-Sr systematics, and do not preclude the possibility of minor disturbances that result in a small but significant change in the slope and therefore apparent date. This is why having many points with a large range in parent/daughter is widely considered necessary for a robust isochron.

One process that could have disturbed the measured ratio of Rb to Sr (and therefore moved the aliquots along the x-axis of the isochron-style diagram) is the analytical approach itself. The leaching experiments done by Shih *et al.* (1998) and Misawa *et al.* (2005) consist of a light agitation in a weak HCl solution. Fractionation of chemical compositions is common during geo- or cosmo-chemical leaching procedures if the entire sample is not digested, particularly when the elements have different chemical behaviour or one is a radiogenic daughter product incompatible in the host (*e.g.*, Mattinson, 1994). This was documented in the experiments by Clauer *et al.* (1993) who leached *ca.* 500 Ma clay minerals in a variety of reagents and measured the Rb-Sr systematics. They demonstrated that 1 mol/L HCl could produce leachates that fractionated Rb and Sr and led to the leachate Rb-Sr and $^{87}Sr/^{86}Sr$ systematics that plotted on linear arrays that did not correspond to accurate ages.

At present, the two tie line slopes from Lafayette and Y000593 are indistinguishable at a ~10 % precision. Whether or not this is a coincidence remains to be seen, and the data indicate that investigating the Rb-Sr systematics of the alteration minerals in the nakhlites might be a fruitful avenue for future work to determine their chronological significance.

Micro-encapsulation $^{40}Ar/^{39}Ar$ Methods

The 0.216 g sample of Lafayette we obtained from the Smithsonian Museum was crushed to 63-125 µm, split into 12 different ~50 mg aliquots, and disaggregated in an ultrasonic bath for 30 minutes, breaking apart grains and separating the iddingsite from their host olivine and pyroxene grains. These grains were examined using a binocular microscope, and any iddingsite adhering to mineral surfaces was scraped off using a fine stainless-steel needle, then manually picked. Aliquots of iddingsite, each weighing *ca.* 1 µg, were prepared for neutron irradiation.

To micro-encapsulate these 12 iddingsite aliquots, we wrapped each aliquot in Cu foil packets positioned within 2 cm-diameter quartz glass tubes, connected to a glass tree on a vacuum line fitted with a glass cold finger. The cold finger was cooled by liquid nitrogen to –196 °C and the glass tube was evacuated. The glass tube was evacuated by a Pfeiffer diaphragm-backed turbomolecular pumping-station and an ion pump (the latter switched on once the system had achieved 10^{-7} mbar). Once a pressure gauge indicated a base pressure better than 2×10^{-9} mbar, the glass tube was flame heated and the sample sealed within the glass capsule. The 12 glass capsules were positioned within a large glass vial along with neutron-fluence monitor Hb3gr (1081.0 ± 1.2 Ma, 1σ; Renne *et al.*, 2011), and secondary standard GA1550 (99.738 ± 0.104 Ma, 1σ; Renne *et al.*, 2011). Samples were then irradiated for 80 hours in the Cd-lined TRIGA facility, Oregon State University, USA.

After a decay period of 4 to 5 months following neutron irradiation, analyses of neutron flux monitors and Lafayette iddingsite aliquots were made in the NERC Argon Isotope Facility, Scottish Universities Environmental Research Centre (SUERC), with a Thermo Scientific HELIX-SFT spectrometer fitted with an ion counting Balzers SEV-217 electron multiplier (measurement of ^{39}Ar-^{36}Ar) and a 10^{12} Ohm resistor Faraday (measurement of ^{40}Ar). Owing to the potential temperature sensitivity of the iddingsite, the material was only baked at 40 °C for 96 hours in an ultra-high vacuum laser cell. Isotope measurements were performed in peak-hopping mode, with a measured sensitivity of 1.13×10^{-13} moles per Volt. Hb3gr crystals were analysed *via* total-fusion and GA1550 crystals were step-heated. All data are reported relative to the J-parameter calculated from measurements of GA1550.

The glass capsules were cracked sequentially in vacuum with a custom-built tube cracker that involves dropping a magnetic ball bearing onto the swan necks of the glass tubes, and the ^{37}Ar and ^{39}Ar was measured. The ^{40}Ar, ^{38}Ar and ^{36}Ar were also measured as a check that neither the bakeout procedure nor the irradiation liberated radiogenic ^{40}Ar from the iddingsite. Beyond small components of terrestrial atmospheric Ar, which is readily detected by its $^{40}Ar/^{36}Ar$ ratio

(Table S-2), there was no evidence of degassing of radiogenic ^{40}Ar. The small copper packets were subsequently extracted from the broken capsules and the samples were fused using a Teledyne 75 W diode laser defocused over the sample using a 2.5 mm spot size and between 30 and 50 % laser power. All released gases were purified using two SAES GP50 getters with ST101 Zr-Al cartridges, one at room temperature and the other at 450 °C. Isotope extraction, purification, extraction line operation and mass spectrometry were fully automated using *MassSpec* software version 8.131.

The ^{37}Ar and ^{39}Ar measurements from the cracked vials were added to the bulk isotope measurements (^{36}Ar-^{40}Ar) and data were corrected for background measurements, mass discrimination, and radioactive decay since irradiation the using *MassSpec* software. The data were also corrected for cosmogenic argon using a combination of the meteorite's cosmogenic exposure age (10.7 ± 0.4 Ma; Cohen *et al.*, 2017), assuming no pre-ejection exposure, and the ^{38}Ar and ^{36}Ar cosmogenic production rates calculated from the Ca/K values measured on each ^{40}Ar/^{39}Ar measurement using the approach of Cassata and Borg (2016), as well as for Martian atmosphere using the trapped ^{40}Ar/^{36}Ar component of 1520 ± 200 (1σ) previously determined by Cohen *et al.* (2017). This measurement was used to correct for Martian atmospheric contribution. The data exhibit a tight clustering on an isotope correlation plot, prohibiting the use of an isochron approach to determine an initial ^{40}Ar/^{36}Ar trapped component composition directly from the iddingsite. We report ages with both analytical precision followed by full external precision, with the latter including uncertainties from the decay constant, at 2-sigma confidence. Ages were calculated using the optimization model of Renne *et al.* (2010) and the parameters of Renne *et al.* (2011). Values used in the ^{40}Ar/^{39}Ar data reduction are listed in Table S-2, and measured argon isotopic data are reported in Table S-3.

The ^{40}Ar/^{39}Ar age we obtain for iddingsite in Lafayette is coincident with most of the initial, low temperature heating steps for the different nakhlites reported by Cohen *et al.* (2017), as is the $^{38}Ar_{Cl}$ enrichment. This observation supports the interpretation that the low temperature extraction steps in most of the bulk rock nakhlite ^{40}Ar/^{39}Ar age spectra define a mixing relationship between a young K-bearing iddingsite and the older magmatic constituents (Fig. S-3). The increasing age with increasing cumulative $^{39}Ar_K$ release is independent of irradiation duration and is correlated with $^{38}Ar_{Cl}$. We know from neutron irradiation of the iddingsite that these samples are susceptible to ^{37}Ar and ^{39}Ar recoil and the significantly younger age steps likely reflect recoil, as previously suggested (Burgess *et al.*, 2000). The observation of young initial age spectra steps associated with alteration of an older igneous rock is also supported by similar distributions in the age spectra of altered terrestrial samples (*e.g.*, Mark *et al.*, 2011). The low temperature diffusive profiles detailed by Cassata *et al.* (2010) for Nakhla are likely masked by the data of Cohen *et al.* (2017) as they did not date pyroxene and plagioclase separates, and instead dated whole rock material, which included a younger iddingsite age component. Moreover, the observation that ^{40}Ar/^{39}Ar ages decrease with increasing $^{38}Ar_{Cl}$ (Fig. S-3), alongside with the good agreement between the ^{40}Ar/^{39}Ar ages of the 12 iddingsite aliquots we measured, argues against the presence of any excess argon in fluid inclusions within the iddingsite (*e.g.*, Harrison *et al.*, 1994; Kelley, 2002).

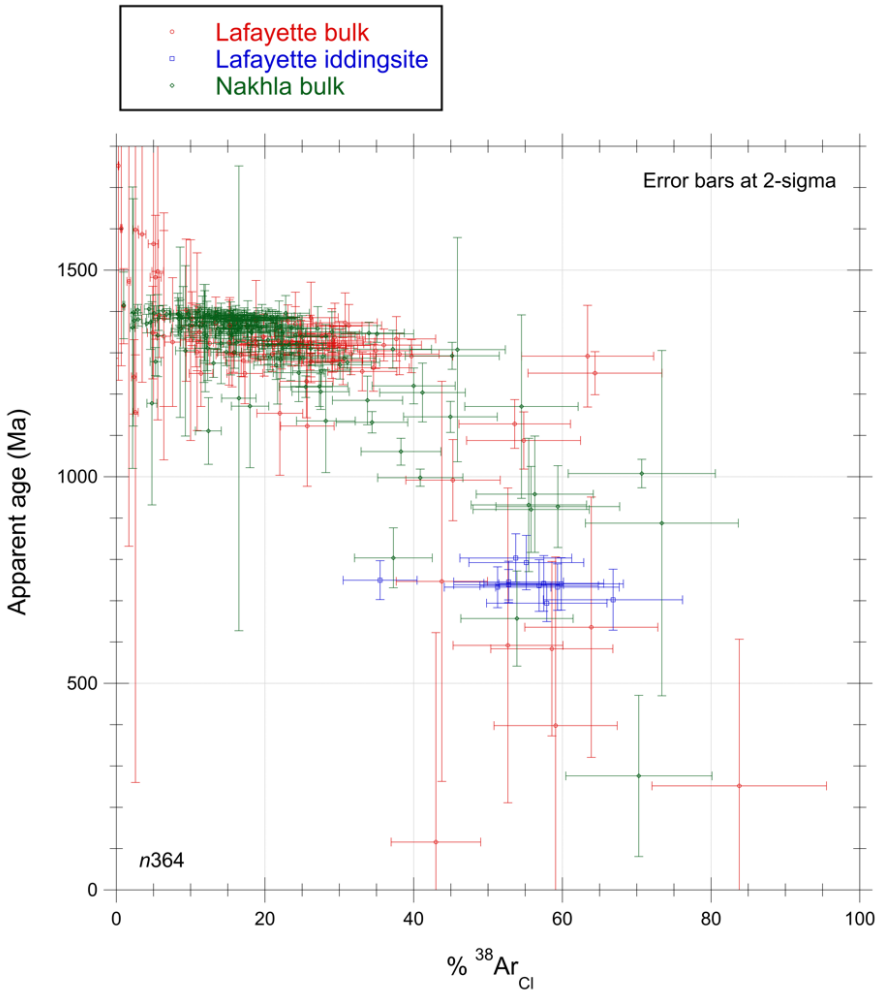

Figure S-3 Apparent $^{40}Ar/^{39}Ar$ age as a function of % $^{38}Ar_{Cl}$ for the Lafayette iddingsite and the bulk-rock step-heating data for Nakhla and Lafayette from Cohen *et al.* (2017). The data show that the low temperature steps from the bulk rock step-heating of Nakhla and Lafayette correlate with the $^{40}Ar/^{39}Ar$ age for the iddingsite as well as the enriched $^{38}Ar_{Cl}$ contents. $^{40}Ar/^{39}Ar$ bulk rock step-heating data yield systematically younger age steps in the first 15 % of ^{39}Ar release and define a mixing relationship between the low-temperature alteration materials and the primary (higher-temperature) igneous component (that defined the age plateaus; Cohen *et al.*, 2017). The youngest ages in the low temperature degassing steps from the bulk measurements are likely an artifact of recoil, as previously suggested (Burgess *et al.*, 2000).

Argon Diffusion Calculations

To evaluate the possibility that different events in the history of Lafayette could have caused partial diffusive loss of radiogenic ^{40}Ar after the iddingsite formed, we performed two different sets of argon diffusion calculations. In the first set of calculations, we model argon diffusive loss for a square pulse heating event, wherein temperature is assumed to instantaneously increase from a temperature below which any diffusion will occur to a constant, higher temperature T (K) for a given duration t (s), and subsequently instantaneously decrease to a temperature below which any diffusion will occur. For this set of calculations, we assume that the duration t of the square pulse heating event is short enough that production of ^{40}Ar by radioactive decay of ^{40}K during the heating event can be ignored. For up to 85 % diffusive loss of argon, the relationship between the fraction of argon lost during such a square pulse heating event and temperature can be expressed as:

$$f \approx \left(\frac{6}{\pi^{\frac{3}{2}}}\right)(\pi^2 F_O)^{\frac{1}{2}} - \left(\frac{3}{\pi^2}\right)(\pi^2 F_O) \quad \text{(S-1)}$$

where F_O, the Fourier number, is equal to:

$$F_O = \frac{D_0 t}{r^2} e^{-E_a/(RT)} \quad \text{(S-2)}$$

and where D_0 is a pre-exponential factor ($cm^2 \cdot s^{-1}$), r is the diffusion length scale (cm) which we assume to be equal to the grain size, E_a is activation energy ($kJ \cdot mol^{-1}$), and R is the gas constant (0.0083145 $kJ \cdot K^{-1} \cdot mol^{-1}$) (McDougall and Harrison, 1999). Equation S-1 can be solved iteratively to determine what temperature, given a specified duration, will produce a given amount of diffusive argon loss. We use these iterative solutions to constrain the duration and temperature combinations that could have caused substantial heating loss from the iddingsite in Lafayette during either its impact ejection event or its atmospheric entry upon falling to Earth, using the diffusion kinetics of muscovite determined experimentally by Harrison *et al.* (2009). We carried out these calculations for two endmember grain sizes (0.01 μm and 10 μm).

In the second set of calculations, we consider a longer-duration event–the 10.7 Myr transit time of Lafayette from its impact ejection from Mars until its atmospheric entry–and therefore do not ignore production of ^{40}Ar by radioactive decay of ^{40}K. Instead, we model the simultaneous production and diffusion of ^{40}Ar under isothermal conditions. These isothermal models represent a reasonable upper bound for the temperatures required to induce partial diffusive loss of the radiogenic argon. This is because for true time-temperature histories along potential orbital trajectories, higher temperatures would be permitted over shorter durations of time. For this set of calculations, we must solve an analytical solution for simultaneous production and diffusion after Wolf *et al.* (1998) that involves two infinite series, which typically converge within 20 partial sums or fewer:

$$t_{app} = \frac{r^2}{D}\left[\frac{1}{15} - \sum_{n=1}^{\infty} \frac{6}{\pi^4 n^4} exp(-n^2\pi^2 F_O)\right] + t_{init} \sum_{n=1}^{\infty} \frac{6}{\pi^2 n^2} exp(-n^2\pi^2 F_O) \quad \text{(S-3)}$$

where t_{app} is the apparent age of the iddingsite (in this case, 742 Ma), and t_{init} is the initial age prior to the onset of isothermal heating (*i.e.* prior to Lafayette's space transit). Like Equation S-1, we can solve Equation S-3 iteratively to map out the grain size and temperature combinations, given an isothermal heating event lasting 10.7 Myr, that would yield a particular fractional argon loss (*i.e.* $1 - t_{app}/t_{init}$). As in the first set of calculations, we used the diffusion kinetics of muscovite determined experimentally by Harrison *et al.* (2009).

Supplementary Tables

Table S-1 Digitized Rb-Sr data from Lafayette (Shih *et al.*, 1998).

Table S-2 Parameter values used in the reduction of $^{40}Ar/^{39}Ar$ data.

Parameter	Value
Isotopic abundances and decay constants (Lee et al., 2006; Renne et al., 2010, 2011)	
$^{40}Ar/^{36}Ar$, Earth's atmosphere	298.56 ± 0.31
$^{40}K/K$	1.167×10^{-4}
$^{40}K\ \lambda_{\varepsilon}$	$(5.757 \pm 0.016) \times 10^{-11}$ a^{-1}
$^{40}K\ \lambda_{\beta}$	$(4.9548 \pm 0.0134) \times 10^{-10}$ a^{-1}
$^{40}K\ \lambda$ total	$(5.5305 \pm 0.0135) \times 10^{-10}$ a^{-1}
$^{37}Ar\ \lambda$	0.01983 ± .0000226 days^{-1}
$^{39}Ar\ \lambda$	$(7.055 \pm 0.039) \times 10^{-6}$ days^{-1}
$^{36}Cl\ \lambda_{\beta}$	$(6.1817 \pm 0.040) \times 10^{-9}$ days^{-1}
Reactor production ratios and interfering isotope production ratios (Renne et al., 2005)	
$(^{36}Cl/^{38}Cl)_{Cl}$	263 ± 2
$(^{38}Ar/^{37}Ar)_{Ca}$	$(1.96 \pm 0.08) \times 10^{-5}$
$(^{38}Ar/^{39}Ar)_{K}$	$(1.22 \pm 0.01) \times 10^{-2}$
$(^{40}Ar/^{39}Ar)_{K}$	$(7.30 \pm 0.92) \times 10^{-4}$
$(^{37}Ar/^{39}Ar)_{K}$	$(2.24 \pm 0.16) \times 10^{-4}$
$(^{39}Ar/^{37}Ar)_{Ca}$	$(6.95 \pm 0.09) \times 10^{-4}$
$(^{36}Ar/^{37}Ar)_{Ca}$	$(2.65 \pm 0.02) \times 10^{-4}$

Table S-3 Argon isotope data from 12 iddingsite aliquots of Lafayette.

Tables S-1 and S-3 are available for download (.xlsx) from the online version of this article at http://doi.org/10.7185/geochemlet.2443.

Supplementary Information References

Bridges, J.C., Grady, M.M. (2000) Evaporite mineral assemblages in the nakhlite (martian) meteorites. *Earth and Planetary Science Letters* 176, 267–279. https://doi.org/10.1016/S0012-821X(00)00019-4

Bridges, J.C., Hicks, L.J., Treiman, A.H. (2019) Carbonates on Mars. In: Filiberto, J., Schwenzer, S.P. (Eds.) *Volatiles in the Martian Crust*. Elsevier, Amsterdam, 89–118. https://doi.org/10.1016/B978-0-12-804191-8.00005-2

Borg, L., Drake, M.J. (2005) A review of meteorite evidence for the timing of magmatism and of surface or near-surface liquid water on Mars. *Journal of Geophysical Research: Planets* 110, E12S03. https://doi.org/10.1029/2005JE002402

Burgess, R., Holland, G., Fernandes, V., Turner, G. (2000) New Ar-Ar Data on Nakhla Minerals. Goldschmidt Conference, 3–8 September 2000, Oxford, UK. *Journal of Conference Abstracts* 5, 266. https://goldschmidtabstracts.info/abstracts/abstractView?id=2000000266

Cassata, W.S., Borg, L.E. (2016) A new approach to cosmogenic corrections in $^{40}Ar/^{39}Ar$ chronometry: Implications for the ages of Martian meteorites. *Geochimica et Cosmochimica Acta* 187, 279–293. https://doi.org/10.1016/j.gca.2016.04.045

Cassata, W.S., Shuster, D.L., Renne, P.R., Weiss, B.P. (2010) Evidence for shock heating and constraints on Martian surface temperatures revealed by $^{40}Ar/^{39}Ar$ thermochronometry of Martian meteorites. *Geochimica et Cosmochimica Acta* 74, 6900–6920. https://doi.org/10.1016/j.gca.2010.08.027

Changela, H.G., Bridges, J.C. (2010) Alteration assemblages in the nakhlites: Variation with depth on Mars. *Meteoritics & Planetary Science* 45, 1847–1867. https://doi.org/10.1111/j.1945-5100.2010.01123.x

Clauer, N., Chaudhuri, S., Kralik, M., Bonnot-Courtois, C. (1993) Effects of experimental leaching on Rb-Sr and K-Ar isotopic systems and REE contents of diagenetic illite. *Chemical Geology* 103, 1–16. https://doi.org/10.1016/0009-2541(93)90287-S

Cohen, B.E., Mark, D.F., Cassata, W.S., Lee, M.R., Tomkinson, T., Smith, C.L. (2017) Taking the pulse of Mars via dating of a plume-fed volcano. *Nature Communications* 8, 640. https://doi.org/10.1038/s41467-017-00513-8

Gyollai, I., Chatzitheodoridis, E., Kereszturi, Á., Szabó, M. (2023) Multiple generation magmatic and hydrothermal processes in a Martian subvolcanic environment based on the analysis of Yamato-000593 nakhlite meteorite. *Meteoritics & Planetary Science* 58, 218–240. https://doi.org/10.1111/maps.13950

Harrison, T.M., Heizler, M.T., Lovera, O.M., Wenji, C., Grove, M. (1994) A chlorine disinfectant for excess argon released from K-feldspar during step heating. *Earth and Planetary Science Letters* 123, 95–104. https://doi.org/10.1016/0012-821X(94)90260-7

Harrison, T.M., Célérier, J., Aikman, A.B., Hermann, J., Heizler, M.T. (2009) Diffusion of ^{40}Ar in muscovite. *Geochimica et Cosmochimica Acta* 73, 1039–1051. https://doi.org/10.1016/j.gca.2008.09.038

Hicks, L.J., Bridges, J.C., Gurman, S.J. (2014) Ferric saponite and serpentine in the nakhlite martian meteorites. *Geochimica et Cosmochimica Acta* 136, 194–210. https://doi.org/10.1016/j.gca.2014.04.010

Kelley, S. (2002) Excess argon in K–Ar and Ar–Ar geochronology. *Chemical Geology* 188, 1–22. https://doi.org/10.1016/S0009-2541(02)00064-5

Krämer Ruggiu, L., Gattacceca, J., Devouard, B., Udry, A., Debaille, V., Rochette, P., Lorand, J.-.-P., Bonal, L., Beck, P., Sautter, V., Busemann, H., Meier, M.M.M., Maden, C., Hublet, G. Martinez, R. (2020) Caleta el Cobre 022 Martian meteorite: Increasing nakhlite diversity. *Meteoritics & Planetary Science* 55, 1539–1563. https://doi.org/10.1111/maps.13534

Lee, J.-Y., Marti, K., Severinghaus, J.P., Kawamura, K., Yoo, H.-S., Lee, J.B., Kim, J.S. (2006) A redetermination of the isotopic abundances of atmospheric Ar. *Geochimica et Cosmochimica Acta* 70, 4507–4512. https://doi.org/10.1016/j.gca.2006.06.1563

Lee, M.R., Tomkinson, T., Mark, D.F., Stuart, F.M., Smith, C.L. (2013) Evidence for silicate dissolution on Mars from the Nakhla meteorite. *Meteoritics & Planetary Science* 48, 224–240. https://doi.org/10.1111/maps.12053

Lee, M.R., Tomkinson, T., Hallis, L.J., Mark, D.F. (2015) Formation of iddingsite veins in the martian crust by centripetal replacement of olivine: Evidence from the nakhlite meteorite Lafayette. *Geochimica et Cosmochimica Acta* 154, 49–65. https://doi.org/10.1016/j.gca.2015.01.022

Lee, M.R., Daly, L., Cohen, B.E., Hallis, L.J., Griffin, S., Trimby, P., Boyce, A., Mark, D.F. (2018) Aqueous alteration of the Martian meteorite Northwest Africa 817: Probing fluid–rock interaction at the nakhlite launch site. *Meteoritics & Planetary Science* 53, 2395–2412. https://doi.org/10.1111/maps.13136

Ludwig, K.R. (2008) Isoplot 3.66: A Geochronological toolkit for Microsoft Excel. *Berkeley Geochronology Center Special Publication* 4, Berkeley.

Mark, D.F., Rice, C.M., Fallick, A.E., Trewin, N.H., Lee, M.R., Boyce, A., Lee, J.K.W. (2011) $^{40}Ar/^{39}Ar$ dating of hydrothermal activity, biota and gold mineralization in the Rhynie hot-spring system, Aberdeenshire, Scotland. *Geochimica et Cosmochimica Acta* 75, 555–569. https://doi.org/10.1016/j.gca.2010.10.014

Martínez, M., Shearer, C.K., Brearley, A.J. (2023) Epitaxial fluorapatite vein in Northwest Africa 998 host apatite: Clues on the geochemistry of late hydrothermal fluids on Mars. *Meteoritics & Planetary Science* 58, 1229–1245. https://doi.org/10.1111/maps.14042

Mattinson, J.M. (1994) A study of complex discordance in zircons using step-wise dissolution techniques. *Contributions to Mineralogy and Petrology* 116, 117–129. https://doi.org/10.1007/BF00310694

McCubbin, F.M., Tosca, N.J., Smirnov, A., Nekvasil, H., Steele, A., Fries, M., Lindsley, D.H. (2009) Hydrothermal jarosite and hematite in a pyroxene-hosted melt inclusion in martian meteorite Miller Range (MIL) 03346: Implications for magmatic-hydrothermal fluids on Mars. *Geochimica et Cosmochimica Acta* 73, 4907–4917. https://doi.org/10.1016/j.gca.2009.05.031

McDougall, I., Harrison, T.M. (1999) *Geochronology and Thermochronology by the $^{40}Ar/^{39}Ar$ Method*. Second Edition, Oxford University Press, New York.

Misawa, K., Shih, C.-Y., Wiesmann, H., Garrison, D.H., Nyquist, L.E., Bogard, D.D. (2005) Rb-Sr, Sm-Nd and Ar-Ar isotopic systematics of Antarctic nakhlite Yamato 000593. *Antarctic Meteorite Research* 18, 133–151.

Nyquist, L.E., Takeda, H., Bansal, B.M., Shih, C.-Y., Wiesmann, H., Wooden, J.L. (1986) Rb-Sr and Sm-Nd internal isochron ages of a subophitic basalt clast and a matrix sample from the Y75011 eucrite. *Journal of Geophysical Research: Solid Earth* 91, 8137–8150. https://doi.org/10.1029/JB091iB08p08137

Piercy, J.D., Bridges, J.C., Hicks, L.J. (2022) Carbonate dissolution and replacement by odinite and saponite in the Lafayette nakhlite: Part of the CO_2-CH_4 cycle on Mars? *Geochimica et Cosmochimica Acta* 326, 97–118. https://doi.org/10.1016/j.gca.2022.02.003

Renne, P.R., Knight, K.B., Nomade, S., Leung, K.-N. Lou, T.-P. (2005) Application of deuteron-deuteron (D-D) fusion neutrons to $^{40}Ar/^{39}Ar$ geochronology. *Applied Radiation and Isotopes* 62, 25–32. https://doi.org/10.1016/j.apradiso.2004.06.004

Renne, P.R., Mundil, R., Balco, G., Min, K., Ludwig, K.R. (2010) Joint determination of ^{40}K decay constants and $^{40}Ar^*/^{40}K$ for the Fish Canyon sanidine standard, and improved accuracy for $^{40}Ar/^{39}Ar$ geochronology. *Geochimica et Cosmochimica Acta* 74, 5349–5367. https://doi.org/10.1016/j.gca.2010.06.017

Renne, P.R., Balco, G., Ludwig, K.R., Mundil, R., Min, K. (2011) Response to the comment by W.H. Schwarz et al. on "Joint determination of ^{40}K decay constants and $^{40}Ar^*/^{40}K$ for the Fish Canyon sanidine standard, and improved accuracy for $^{40}Ar/^{39}Ar$ geochronology" by P.R. Renne et al. (2010). *Geochimica et Cosmochimica Acta* 75, 5097–5100. https://doi.org/10.1016/j.gca.2011.06.021

Rotenberg, E., Davis, D.W., Amelin, Y., Ghosh, S., Bergquist, B.A. (2012) Determination of the decay-constant of ^{87}Rb by laboratory accumulation of ^{87}Sr. *Geochimica et Cosmochimica Acta* 85, 41–57. https://doi.org/10.1016/j.gca.2012.01.016

Shih, C.-Y., Nyquist, L.E., Reese, Y., Wiesmann, H. (1998) The Chronology of the Nakhlite, Lafayette: Rb-Sr and Sm-Nd Isotopic Ages. *Lunar and Planetary Science Conference XXIX*, abstract 1145.

Shih, C.-Y., Nyquist, L.E., Wiesmann, H. (1999) Samarium-neodymium and rubidium-strontium systematics of nakhlite Governador Valadares. *Meteoritics & Planetary Science* 34, 647–655. https://doi.org/10.1111/j.1945-5100.1999.tb01370.x

Shih, C.Y., Wiesmann, H., Nyquist, E.L. Misawa, K. (2002) Crystallization age of Antarctic nakhlite Y000593: Further evidence of nakhlite launch pairing. *Antarctic Meteorites XXVII*, 151–153.

Steiger, R.H., Jäger, E. (1977) Subcommission on geochronology: Convention on the use of decay constants in geo- and cosmochemistry. *Earth and Planetary Science Letters* 36, 359–362. https://doi.org/10.1016/0012-821X(77)90060-7

Tomkinson, T., Lee, M.R., Mark, D.F., Smith, C.L. (2013) Sequestration of Martian CO_2 by mineral carbonation. *Nature Communications* 4, 2662. https://doi.org/10.1038/ncomms3662

Treiman, A.H. (2005) The nakhlite meteorites: Augite-rich igneous rocks from Mars. *Geochemistry* 65, 203–270. https://doi.org/10.1016/j.chemer.2005.01.004

Treiman, A.H., Barrett, R.A., Gooding, J.L. (1993) Preterrestrial aqueous alteration of the Lafayette (SNC) meteorite. *Meteoritics* 28, 86–97. https://doi.org/10.1111/j.1945-5100.1993.tb00251.x

Vermeesch, P. (2018) IsoplotR: A free and open toolbox for geochronology. *Geoscience Frontiers* 9, 1479–1493. https://doi.org/10.1016/j.gsf.2018.04.001

Wolf, R.A., Farley, K.A., Kass, D.M. (1998) Modeling of the temperature sensitivity of the apatite (U–Th)/He thermochronometer. *Chemical Geology* 148, 105–114. https://doi.org/10.1016/S0009-2541(98)00024-2

York, D., Evensen, N.M., Martínez, M.L., De Basabe Delgado, J. (2004) Unified equations for the slope, intercept, and standard errors of the best straight line. *American Journal of Physics* 72, 367–375. https://doi.org/10.1119/1.1632486